

# Identification of Surface Markers and Functional Characterization of Myeloid Derived Suppressor Cell-Like Adherent Cells

John Clyde Co Soriano, Shiho Tsutsumi, Daiya Ohara, Keiji Hirota, Gen Kondoh, Tatsuya Niwa, Hideki Taguchi, Tetsuya Kadonosono,\* and Shinae Kizaka-Kondoh

Myeloid-derived suppressor cell (MDSC)-like adherent cells (MLACs) are a recently identified CD11b<sup>+</sup>F4/80<sup>-</sup> myeloid cell subset that can infiltrate tumors early in development and promote their growth. Because of these functions, MLACs play an important role in establishing an immunosuppressive tumor microenvironment (TME). However, the lack of MLAC-specific markers has hampered further characterization of this cell type. This study identifies the gene signature of MLACs by analyzing RNA-sequencing (RNA-seq) and public single-cell RNA-seq data, revealing that MLACs are an independent cell population that are distinct from other intratumoral myeloid cells. After combining proteome analysis of membrane proteins with RNA-seq data, H2-Ab1 and CD11c are indicated as marker proteins that can support the isolation of MLAC subsets from CD11b<sup>+</sup>F4/80<sup>-</sup> myeloid cells by fluorescence-activated cell sorting. The CD11b<sup>+</sup>F4/80<sup>-</sup>H2-Ab1<sup>+</sup> and CD11b<sup>+</sup>F4/80<sup>-</sup>CD11c<sup>+</sup> MLAC subsets represent approximately half of the MLAC population that is isolated based on their adhesion properties and possess gene signatures and functional properties similar to those of the MLAC population. Additionally, membrane proteome analysis suggests that MLACs express highly heterogeneous surface proteins. This study facilitates an integrated understanding of heterogeneous intratumoral myeloid cells, as well as the molecular and cellular details of the development of an immunosuppressive TME.

## 1. Introduction

Myeloid cells are a highly diverse immune cell population that abundantly infiltrates tumors and contributes to the development of a complex tumor microenvironment (TME). Among them, myeloid-derived suppressor cells (MDSCs)<sup>[1]</sup> are immature and heterogeneous populations that expand systemically in individuals with cancer. MDSCs are defined as key regulators of an immunosuppressive TME. MDSC-mediated immunosuppression occurs mainly from the release of reactive oxygen species (ROS) and upregulation of inducible nitric oxide synthase and arginase 1 expression levels.<sup>[2,3]</sup> MDSCs are CD11b<sup>+</sup>Gr-1<sup>+</sup> cell populations that can be subdivided into two major subsets: CD11b<sup>+</sup>Ly6C<sup>int/-</sup>Ly6G<sup>+</sup> polymorphonuclear MDSCs (PMN-MDSCs) and CD11b<sup>+</sup>Ly6C<sup>+</sup>Ly6G<sup>int/-</sup> monocytic MDSCs (M-MDSCs).<sup>[3,4]</sup> M-MDSCs can differentiate into tumor-associated macrophages (TAMs), which are also highly heterogeneous and exhibit apparent phenotypic plasticity.<sup>[5,6]</sup> TAMs can be distinguished from MDSCs by their F4/80 expression and strong adherence to plastic culture dishes.<sup>[5,7,8]</sup>

J. C. Co Soriano, S. Tsutsumi, T. Kadonosono, S. Kizaka-Kondoh  
School of Life Science and Technology  
Tokyo Institute of Technology  
Yokohama 226–8501, Japan  
E-mail: [tetsuyak@bio.titech.ac.jp](mailto:tetsuyak@bio.titech.ac.jp)

D. Ohara, K. Hirota, G. Kondoh  
Institute for Frontier Life and Medical Sciences  
Kyoto University  
Sakyo-Ku, Kyoto 606–8507, Japan  
T. Niwa, H. Taguchi  
Institute for Innovative Research  
Tokyo Institute of Technology  
Yokohama 226–8503, Japan

 The ORCID identification number(s) for the author(s) of this article can be found under <https://doi.org/10.1002/adbi.202300159>

© 2023 The Authors. Advanced Biology published by Wiley-VCH GmbH. This is an open access article under the terms of the [Creative Commons Attribution-NonCommercial-NoDerivs](#) License, which permits use and distribution in any medium, provided the original work is properly cited, the use is non-commercial and no modifications or adaptations are made.

DOI: 10.1002/adbi.202300159

MDSC-like adherent cells (MLACs) are recently identified F4/80-negative myeloid cells that were isolated based on their property of strongly adhering to plastic dishes. MLACs are similar to MDSCs in terms of cell surface marker expression and division into Ly6C<sup>hi</sup>Ly6G<sup>-</sup> and Ly6C<sup>low</sup>Ly6G<sup>+</sup> subsets, but differ in function: MLACs are not immunosuppressive and can directly promote tumor growth.<sup>[8]</sup> Because MLACs infiltrate early-stage tumors and recruit MDSCs by secreting cytokines, it has been suggested that MLACs can contribute to the development of an immunosuppressive TME. However, MLAC-specific surface markers have not been identified and *in vivo* studies on the precise functions of MLACs have been limited.

Recent studies using comprehensive analyses with single-cell resolution have provided a clearer picture of heterogeneous myeloid cells,<sup>[9–11]</sup> bringing gene signature-based definition of cells toward morphologically and phenotypically named MDSC populations.<sup>[4]</sup> These analyses revealed that there are many unidentified cell populations with gene signatures distinct from those previously identified by surface marker proteins. As myeloid cells are highly plastic and difficult to classify as distinct cell populations, it is crucial to identify and functionally dissect cell populations that exhibit context-dependent phenotypes to better understand the complexity of the TME. Therefore, public single-cell RNA-sequencing (scRNA-seq) data provide extremely useful information for analyzing uncharacterized cell populations, accelerating the elucidation of these highly plastic cell populations.

In this study, we investigated the molecular features and cell surface markers of MLACs by comparing them with MDSCs using a combination of RNA-sequencing (RNA-seq) and membrane proteomics analyses. RNA-seq analysis showed that MLACs have a specific gene signature that is distinct from those of MDSCs and TAMs. By analyzing public scRNA-seq data, we could identify clusters with MLAC gene signatures. This integrated analysis allowed us to identify two surface markers that separate MLAC subsets from a CD11b<sup>+</sup>F4/80<sup>-</sup> population containing MLACs and MDSCs by fluorescence-activated cell sorting: Histocompatibility 2, class II antigen A, beta 1 (H2-Ab1), a major histocompatibility complex (MHC) II subunit,<sup>[12]</sup> and integrin alpha X, also known as CD11c.<sup>[13]</sup> The population of CD11b<sup>+</sup>F4/80<sup>-</sup>H2-Ab1<sup>+</sup> and CD11b<sup>+</sup>F4/80<sup>-</sup>CD11c<sup>+</sup> cells showed the same gene signature and functions as MLACs isolated on the basis of their strong adhesion properties, indicating that they are representative MLAC subpopulations. Studies using these markers will facilitate further characterization of MLAC functions *in vivo* and contribute to an integrated understanding of myeloid cell functions in the TME.

## 2. Results

### 2.1. MLACs Have a Transcriptome Profile Distinct from MDSCs and TAMs

Single-cell suspensions containing MDSCs, MLACs, and TAMs were prepared from Lewis lung carcinoma (LCC) tumors and separated into adherent and non-adherent fractions based on their adherence properties to culture dishes (adhesion-based separation, see Methods). MLACs and TAMs were then separated from the adherent fraction as CD11b<sup>+</sup>F4/80<sup>-</sup> and CD11b<sup>+</sup>F4/80<sup>+</sup>

populations, respectively, and MDSCs were separated from the non-adherent fraction as a CD11b<sup>+</sup>Gr-1<sup>+</sup> population using fluorescence-activated cell sorting (FACS) (Figure 1A; Figure S1, Supporting Information). RNA-seq analysis of these cells demonstrated that MLACs, TAMs, and MDSCs have unique gene expression profiles. Hierarchical clustering analysis showed that the transcriptome profile between MDSCs and TAMs was more similar than that of MDSCs and MLACs (Figure 1B; Figure S2A, Supporting Information). These results clearly indicate that MLACs are a distinct population from MDSCs and TAMs. For cell type-specific markers, MLACs and TAMs could be clearly separated from each other through F4/80 expression, but no suitable marker exists to distinguish between MLACs and MDSCs. Therefore, we focused on comparing the transcriptomic details of MLACs and MDSCs to elucidate the molecular differences between these cells. There were 348 and 2331 genes with at least two-fold higher and lower expression levels, respectively, in MLACs compared with MDSCs (Figure 1C). Gene set enrichment analysis (GSEA) suggested that MLACs are involved in unique biological processes compared with MDSCs, including inflammation through cytokine production and granulocyte migration (Figure S2B, Supporting Information). These results support the previous finding that MLACs can recruit MDSCs through specific secreted factors.

Because MLACs and MDSCs display different adhesion properties, differentially expressed genes encoding plasma membrane proteins (GO: 0005886) were analyzed using QuickGO's gene ontology (GO) database.<sup>[14]</sup> After focusing on plasma membrane encoding genes among the differentially expressed genes, 56 genes in total were expressed at least two-fold higher in MLACs than in MDSCs. In contrast, 102 plasma membrane protein genes in total were expressed at least two-fold less in MLACs than in MDSCs (Figure 1D). We searched for potential MLAC markers by selecting plasma membrane genes that were strongly upregulated in MLACs and had high transcript counts. The highly upregulated surface marker genes included adhesion proteins, like Selp and Sell, MHC-associated proteins, like CD74, H2-Eb1, and H2-Q10, and cytokine receptors, like CXCR1, CXCR2, and CCRL2 (Figure 1E; Table S1, Supporting Information). RNA-seq analysis revealed that the most upregulated membrane protein genes in MLACs were *CD209a* (DC-SIGN), *Ctsk* (Cathepsin K), and *H2-Dmb2* (histocompatibility 2, class II, locus Mb2). These transcriptome analyses confirm that MLACs are a distinct myeloid cell population from MDSCs and TAMs, highlighting MLAC-specific surface marker candidates.

### 2.2. Identification of an MLAC Gene Signature in Public scRNA-Seq Data

To further explore the gene signature of MLACs, public scRNA-seq data were examined for cells with similar gene expression patterns to those of MLACs, MDSCs, and TAMs observed in our RNA-seq analysis. The scRNA-seq data set<sup>[15]</sup> composed of syngeneic mouse tumors, such as B16-F10 (melanoma), CT26 (colon), EMT6 (breast cancer), LLC (lung), MC38 (colon), and SA1N (fibrosarcoma), was analyzed for tumor-infiltrating immune cells. To confirm the presence of MLACs in the scRNA-seq

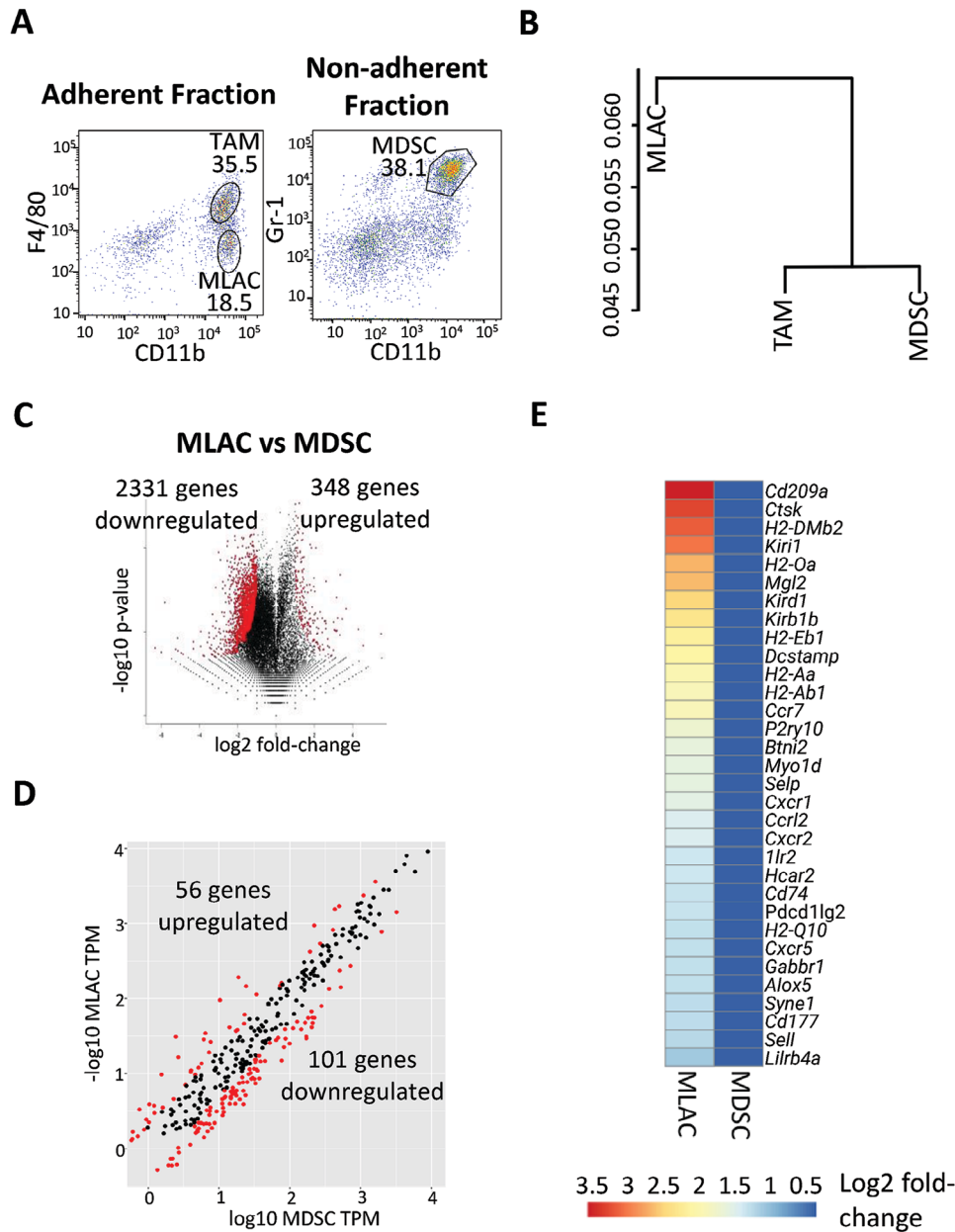


**Figure 1.** Analysis of differences in gene expression profiles of MDSCs and MLACs. A) Immunophenotyping of MLACs, TAMs, and MDSCs for sorting. B) Hierarchical clustering analysis of MLACs, TAMs, and MDSCs based on differences in gene expression profiles obtained via RNA-sequencing (RNA-seq). C) Volcano plot of RNA-seq analysis between MLACs and MDSCs. Red dots indicate genes that were differentially expressed in MLACs or MDSCs. D) Scatterplot of normalized transcript counts of plasma membrane encoding genes between MLACs and MDSCs. Red dots indicate genes that were upregulated or downregulated at least two-fold in MLACs compared with MDSCs. E) Heatmap of the top 32 genes encoding plasma membrane proteins that were differentially expressed in MLACs compared with MDSCs. Gene expression was normalized to log<sub>2</sub> fold-change.  $n = 1$ .

data, the CD11b<sup>+</sup>F4/80<sup>-</sup> population, containing MLACs and MDSCs, was first defined as high expression of *Itgam* (CD11b) and low expression of *Adgre1* (F4/80) (Figure S3A, Supporting Information). We subsetted and analyzed the CD11b<sup>+</sup>F4/80<sup>-</sup> cells and identified five distinct clusters (clusters 1 to 5) (Figure S3A, Supporting Information). To identify MLAC, M-MDSC, and PMN-MDSC clusters, we first identified the monocytic and granulocytic populations. Clusters 1, 3, and 5 expressed the monocyte markers *Mafb* and *Ccr2*,<sup>[11,16]</sup> while cluster 4 expressed

the neutrophil marker *Csf3r*.<sup>[17]</sup> Cluster 2 only had low expression of *Ccr2* (Figure 2A). These findings suggest that clusters 1, 3, and 5 were monocytic cells, while cluster 4 was granulocytic cells.

We then analyzed the differentially expressed genes in each cluster to determine the top marker genes for each. We utilized the upregulated marker genes from our RNA-seq results to identify the MLAC cluster (Figure 2B). Cluster 2 uniquely expressed *Cd209a*, *Klr1d1*, *Cd74*, *Il1r2*, and *Mgl2*, which were

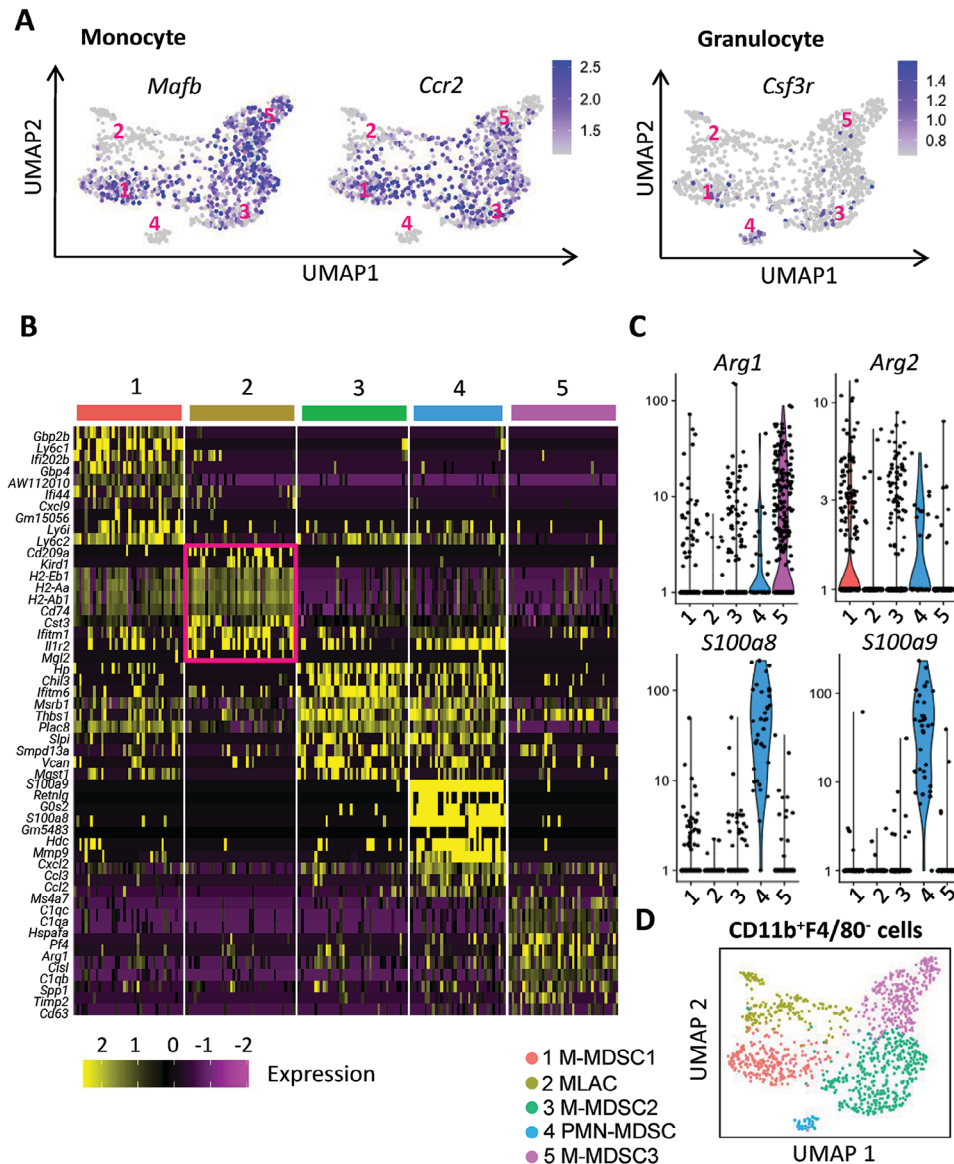


**Figure 2.** Identification of a MLAC gene signature using RNA-seq and public scRNA-seq data. The Kumar et al. dataset was analyzed using Seurat. CD11b<sup>+</sup>F4/80<sup>-</sup> cells were subsetted and divided into five distinct clusters. A) Monocytes were outlined based on *Ccr2* and *Mafb* expression, while granulocytes were outlined based on *Csf3r* expression. B) Heatmap summary of the top 10 marker genes identified for each CD11b<sup>+</sup>F4/80<sup>-</sup> cluster of Seurat analysis. The MLAC cluster is boxed in red. C) Violin plot showing the differential expression of immunosuppressive factors between CD11b<sup>+</sup>F4/80<sup>-</sup> clusters. D) UMAP plot of CD11b<sup>+</sup>F4/80<sup>-</sup> cells with cluster names identified.

also significantly upregulated in MLACs in the RNA-seq analysis (Figures 1E and 2B). We determined the MDSC clusters using a combination of immunosuppressive factors and MDSC marker genes and clarified their distinction from MLACs. In general, all the other subsets had higher expression levels of immunosuppressive factors compared with cluster 2. Arginase (*Arg1*) was highly expressed in clusters 4 and 5, while *Arg2*<sup>[18]</sup> was highly expressed in clusters 1, 3, and 4. Furthermore, cluster 4 had the highest expression levels of *S100a8*/*S100a9* (Figure 2C), the genes encoding the S100 calcium-binding proteins *S100a8* and *S100a9*,<sup>[19,20]</sup> respectively. These proteins are known to be involved in the immunosuppressive and pro-tumorigenic functions of PMN-MDSCs.<sup>[19,20]</sup> These data

suggest that all the CD11b<sup>+</sup>F4/80<sup>-</sup> cells except cluster 2 possess some immunosuppressive capacity. Clusters 1, 3, 4, and 5 expressed several MDSC marker genes, such as *Cd33*, *Clec4d*, *Clec4e*, *Cd84*, *Ctsd*, and *Cd300la*,<sup>[9,21]</sup> while cluster 2 showed lower expression levels of these genes (Figure S3B, Supporting Information). From these analyses, clusters 1, 3, and 5 were defined as M-MDSCs because they are monocytic populations (Figure 2A), cluster 4 was defined as PMN-MDSCs, and cluster 2 was defined as MLACs from their lack of expression of immunosuppressive factors and MDSC marker gene expression (Figure 2D; Figure S3B, Supporting Information). Figure 2D summarizes this analysis and how the clusters were defined. Based on the UMAP clustering, the MLAC cluster appears to

be more related to the M-MDSC clusters than the PMN-MDSC cluster.

Because the upregulation of *Cd209a*, *Klrd1*, *Cd74*, *Il1r2*, and *Mgl2* in MLACs was observed in both our RNA-seq and scRNA-seq public data analyses, we considered these genes to be MLAC signature genes and used them as a tool to identify MLAC populations. We used qRT-PCR to compare the expression patterns of the MLAC signature genes between MLACs and MDSCs isolated using the adhesion method (Figure S3C, Supporting Information) and validated that these genes were all upregulated in MLACs compared with MDSCs.

The consistency of the MLAC gene signature was confirmed by analysis using another public scRNA-seq dataset, which focused on B16-F10 tumors.<sup>[22]</sup> We identified the CD11b<sup>+</sup>F4/80<sup>-</sup> cell populations by gene expression analysis (Figure S4A, Supporting Information). Cluster 2 highly expressed MLAC signature genes and other top MLAC marker genes and had low expression of genes encoding immunosuppressive factors (Figure S4B, Supporting Information). Cluster 2 also had low expression of MDSC signature genes (Figure S4C, Supporting Information), and was defined as MLAC (Figure S4D, Supporting Information). Taken together, these results indicated that MLACs are a myeloid cell population commonly present within tumors and indeed distinct from MDSCs.

### 2.3. Integration of Membrane Proteome and Transcriptome Analyses to Determine Marker Proteins for MLAC Isolation

Importantly, the mRNA expression levels of a gene do not necessarily reflect the corresponding protein levels.<sup>[23]</sup> Membrane proteins from MLACs and MDSCs that were isolated by adhesion-based separation and FACS were subjected to shotgun MS analysis through a label-free quantitative proteomics approach. A total of 1506 proteins were reproducibly identified in each sample. Differentially expressed proteins at high levels (>three-fold) between the samples were selected (Figure 3A). Proteins expressed higher in MLACs than in MDSCs were Class II histocompatibility antigen, M alpha chain (H2-Dma), CD11c, H2-Ab1, H-2 class II E-D beta chain, Trpv2, H-2 class II I-E alpha chain (H2-Eb1), CD74, Vamp7, H2-Aa, Ceacam1, and Rars2. Proteins expressed higher in MDSCs than in MLACs were CD93, Ighg, Endod1, Fcgr1, and Hmgh2.

Rank-rank hypergeometric overlap (RRHO) analysis<sup>[24]</sup> was performed to select high-confidence markers and validate the correlated hits between the transcriptome and proteome analyses. Composite ranks were determined based on the highest fold-change and lowest *p*-value from differentially expressed genes and proteins. *Mgl2* (CD301a), H2-Eb1, H2-Aa, H2-Ab1, CD74, and CD11c were ranked as the top six most consistent proteins between both datasets (Figure 3B; Table S3, Supporting Information).

Six candidate proteins were investigated to determine which proteins would be suitable markers for isolating MLACs from CD11b<sup>+</sup>F4/80<sup>-</sup> populations by flow cytometry using commercially available antibodies (Figure 3C,D). A significant population of MLACs obtained by adhesion-based separation (hereafter referred to as Adh-MLACs) expressed H2-Ab1 and CD11c, while

only a small population expressed CD74. In contrast, MDSCs did not express any of these markers. Flow cytometry analysis revealed that ≈44% of Adh-MLACs were labeled using antibodies against H2-Ab1 and CD11c. Approximately 30% and 28% of Adh-MLACs were labeled with H2-Ab1 and CD11c antibodies, respectively, of which ≈13% to 16% were double-positive (Figure 3E). These results indicate that, although we were unable to identify cell surface marker capable of labeling all MLACs, we can use H2-Ab1 and CD11c as markers to directly isolate MLAC subsets from the tumor-extracted CD11b<sup>+</sup>F4/80<sup>-</sup> populations.

### 2.4. Analysis of H2-Ab1- and CD11c-Positive MLAC Subsets

Currently, MLACs are separated from MDSCs based on their different adherent properties to plastic dishes. Tumor-extracted cells are first divided into adherent and non-adherent fractions and then separated using known markers (Figure S1, Supporting Information). MLAC subsets were isolated directly from tumor-extracted CD11b<sup>+</sup>F4/80<sup>-</sup> populations based on H2-Ab1 and CD11c expression (Figure 4A; Figure S5, Supporting Information). The H2-Ab1<sup>+</sup> and CD11c<sup>+</sup> cells gated from CD11b<sup>+</sup>F4/80<sup>-</sup> cells comprised ≈15% and 13%, respectively, of the FACS-separated CD11b<sup>+</sup>F4/80<sup>-</sup> population (Figure 4A). These percentages were about half of those gated from the Adh-MLACs (Figure 3E). To validate the molecular characteristics of these cells, CD11b<sup>+</sup>F4/80<sup>-</sup>H2-Ab1<sup>+</sup> and CD11b<sup>+</sup>F4/80<sup>-</sup>CD11c<sup>+</sup> cells (hereafter abbreviated as H2-Ab1<sup>+</sup> and CD11c<sup>+</sup>, respectively, and their negative counterparts as H2-Ab1<sup>-</sup> and CD11c<sup>-</sup>) were sorted directly from tumor single-cell suspensions and analyzed for expression of the MLAC signature genes. Expression levels of *Mgl2*, *Cd209a*, *Klrd1*, and *Cd74* were highly elevated in Adh-MLACs, H2-Ab1<sup>+</sup> cells, and CD11c<sup>+</sup> cells, but low in H2-Ab1<sup>-</sup> cells, CD11c<sup>-</sup> cells, and MDSCs isolated from the non-adherent fraction (NA-MDSC) (Figure 4B).

H2-Ab1<sup>+</sup> and CD11c<sup>+</sup> MLAC subsets were investigated for functional characteristics of MLACs: direct growth promotion and lack of immunosuppression.<sup>[8]</sup> H2-Ab1<sup>+</sup> and CD11c<sup>+</sup> cells showed significant LLC growth-promoting activity to a similar extent as Adh-MLACs, while H2-Ab1<sup>-</sup> and CD11c<sup>-</sup> cells showed weak growth-promoting activity similar to NA-MDSCs (Figure 4C). The immunosuppressive activities of MLACs and MDSCs were examined by a coculture immunosuppression assay, in which Adh-MLACs and NA-MDSCs were cocultured with polyclonally stimulated CD8<sup>+</sup> T cells. T cell proliferation rates were examined by Carboxyfluorescein succinimidyl diester (CFSE) dilution. Our data suggest that Adh-MLACs did not suppress T cell proliferation, while NA-MDSCs showed significant suppression of T cell proliferation (Figure 4D), confirming the T cell immunosuppressive activity of MDSCs and lack of such activity in MLACs.<sup>[8]</sup> When H2-Ab1<sup>+</sup> cells, CD11c<sup>+</sup> cells, and their corresponding negative marker populations were examined for immunosuppressive activity, CD8<sup>+</sup> T cell proliferation was not affected by H2A1b<sup>+</sup> or CD11c<sup>+</sup> cells, but was significantly inhibited by H2-Ab1<sup>-</sup> and CD11c<sup>-</sup> cells (Figure 4E), indicating that H2-Ab1<sup>+</sup> and CD11c<sup>+</sup> cells lack T cell immunosuppressive activities. These results confirmed that the H2A1b<sup>+</sup> and CD11c<sup>+</sup> subsets possess the functional properties of MLACs.

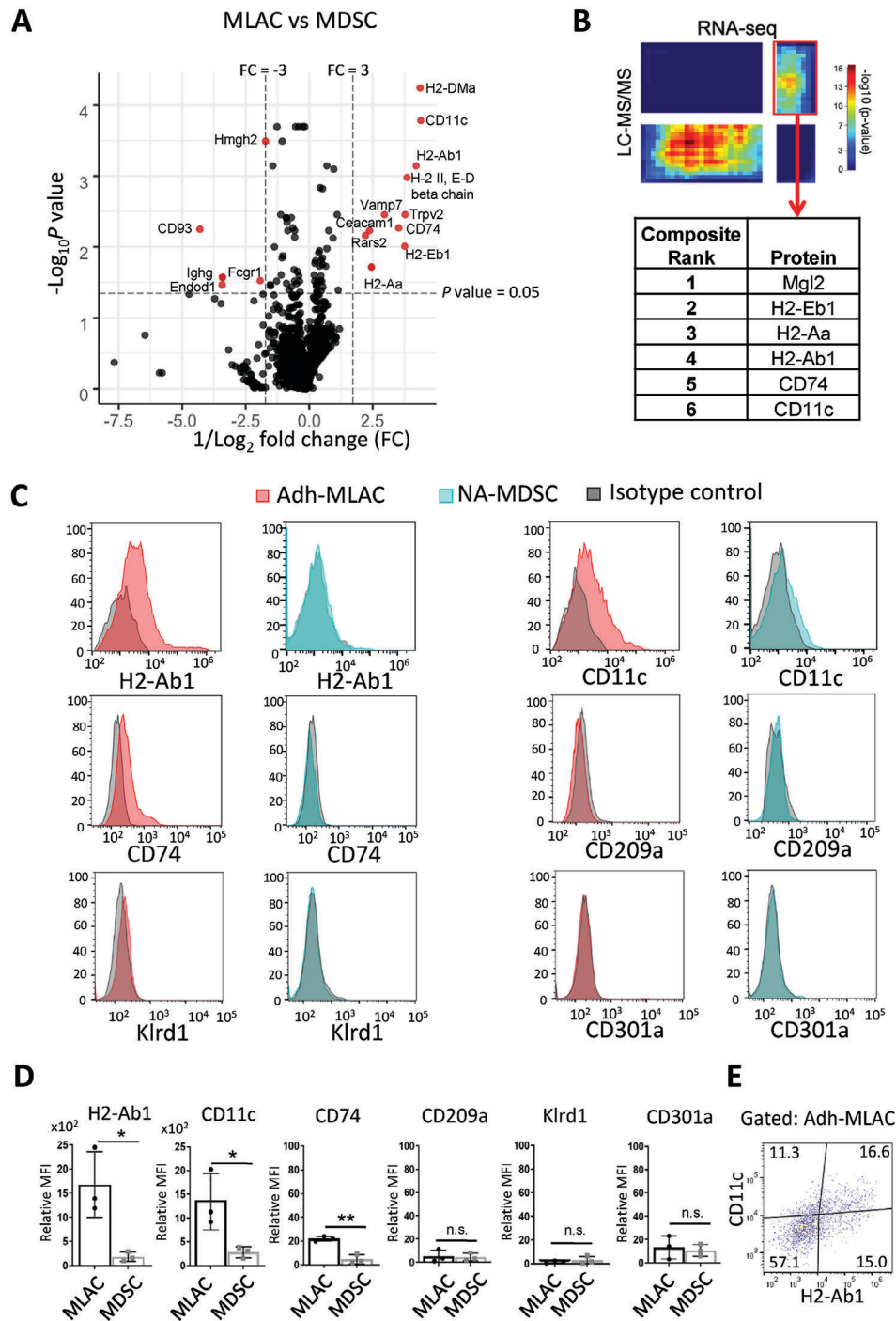


**Figure 3.** Proteome analysis and screening of candidate cell surface markers. A) Volcano plot showing the top differentially expressed proteins between MDSCs and MLACs from quantitative liquid chromatography-tandem mass spectrometry (LC-MS/MS) analysis. X and y dashed lines indicate upregulation for either MLACs or MDSCs with fold-change (FC) > 3 and  $P > 0.05$ , respectively. Red dots with protein names indicate significantly upregulated candidate proteins.  $n = 3$ .  $p$ -values were calculated using an unpaired Student's  $t$ -test. B) RRHO heatmap comparing rank overlap of differentially expressed membrane genes and membrane proteins. The upper right quadrant indicates genes and proteins that were upregulated in MLACs compared with MDSCs in both datasets. Red and blue indicate the highest and lowest degree of overlap, respectively. The list below the heatmap shows the top six ranked proteins with the most correlated protein and mRNA expression levels in the upper right quadrant of the RRHO heatmap. C) MLACs were gated as  $CD11b^+ F4/80^-$  from the Adherent fraction (Adh-MLACs), while MDSCs were gated as  $CD11b^+ Gr-1^+$  from the non-adherent fraction (NA-MDSCs). Expression levels of marker candidates in Adh-MLACs and NA-MDSCs were analyzed by flow cytometry. D) Relative mean fluorescence intensity (MFI) of the results in panel C are shown. Relative MFI =  $MFI_{\text{stained sample}} - MFI_{\text{isotype control}}$ . E) Flow cytometry analysis of H2-Ab1 and CD11c expressing populations of Adh-MLAC. Data are presented as mean  $\pm$  SD,  $n = 3$ .  $p$ -values were calculated using an unpaired Student's  $t$ -test. \*  $p < 0.05$ , \*\*  $p < 0.01$ , n.s., not significant.

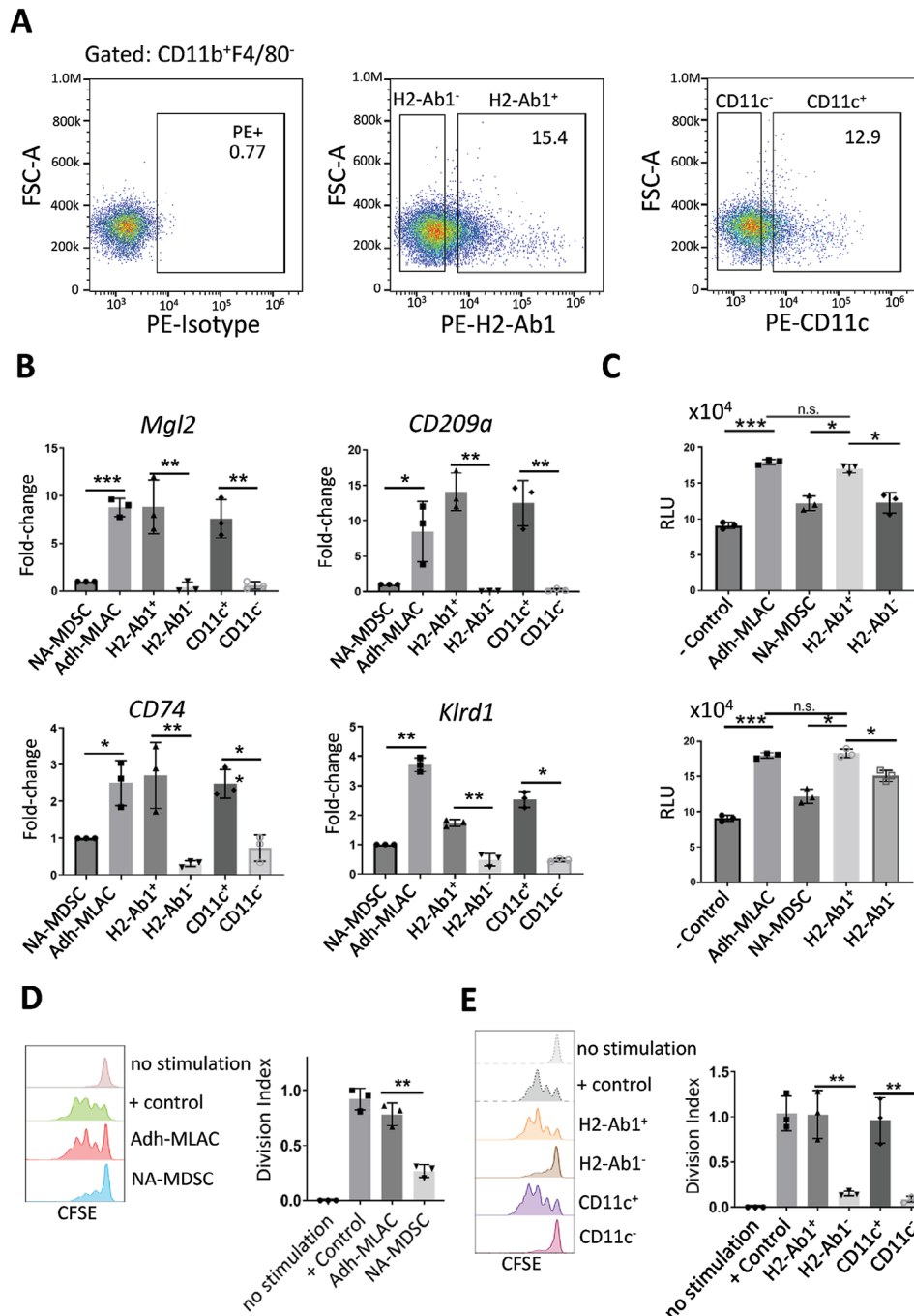


**Figure 4.** Isolation and analysis of H2-Ab1<sup>+</sup> or CD11c<sup>+</sup> MLAC subsets. A) CD11b<sup>+</sup>F4/80<sup>-</sup> cells gated in Figure S5 (Supporting Information) were analyzed for H2-Ab1 (middle) and CD11c (right) expression by flow cytometry. Positive gates were set based on isotype controls (left). B) H2-Ab1<sup>+</sup> cells, CD11c<sup>+</sup> cells, CD11c<sup>-</sup> cells, Adh-MLACs, and NA-MDSCs were sorted by FACS and subjected to qRT-PCR analysis. Expression levels of target genes were normalized to actin and fold-change of target cell population over MDSC expression was calculated. Representative MLAC signature genes were confirmed to be consistently upregulated in Adh-MLACs, H2-Ab1<sup>+</sup> cells, and CD11c<sup>+</sup> cells compared with NA-MDSCs or H2-Ab1<sup>-</sup> and CD11c<sup>-</sup> cells. C) Direct growth-promoting effects of H2-Ab1<sup>+</sup> (left) and CD11c<sup>+</sup> (right) on cancer cells. LLC/Fluc cells were cocultured with test cells. After coculture for 48 h, the luciferase activity of the LLC/Fluc cells was measured. The growth rate of LLC/Fluc cells without coculture was indicated as – Control. Relative LLC/Fluc cell growth is shown as relative luminescence units (RLUs). D, E) CFSE-labeled and stimulated CD8<sup>+</sup> T cells were cocultured with Adh-MLACs or NA-MDSCs D) and with H2-Ab1<sup>+</sup> cells or CD11c<sup>+</sup> cells E). T cell proliferation was analyzed by flow cytometry and indicated by division index. B–E), Data are presented as mean ± SD, *n* = 3. *p*-values were calculated using unpaired Student's *t*-test \* *p* < 0.05, \*\* *p* < 0.01, \*\*\* *p* < 0.001, n.s., not significant.

### 3. Discussion

In this study, we combined public scRNA-seq data analysis with transcriptome and membrane proteome analyses to reveal that MLACs are a distinct cell population from MDSCs and TAMs. Additionally, we found that H2-Ab1 and CD11c are MLAC-specific surface marker proteins that allow the separation of MLAC subsets from tumor-extracted CD11b<sup>+</sup>F4/80<sup>-</sup> cell populations.

From our RNA-seq data analysis, we identified the genes that were uniquely expressed by MLACs: *Mgl2*, *CD209a*, *CD74*, and *Klrd1*. These genes form the MLAC gene signature that can be used to distinguish MLACs from other CD11b<sup>+</sup>F4/80<sup>-</sup> cells in tumors. The majority of the top upregulated genes in MLACs are biologically involved in antigen presentation, like *CD74* and *H2-Ab1*, or have been associated with dendritic cells, such as *Mgl2* and *CD209a*.<sup>[25]</sup> This suggests that MLACs may have functions in the auxiliary regulation of immune responses.

GO enrichment analysis of RNA-seq data of MDSCs and MLACs suggested that several biological processes, such as cytokine production and granulocyte migration, were more active in MLACs compared with MDSCs. High expression levels of *CXCL1*, *CXCL2*, *CXCR1*, and *CXCR2* in MLACs (Table S2, Supporting Information) suggest that activation of the CXCR1-CXCR2/CXCL8 axis is involved in MDSC recruitment and tumor growth,<sup>[26]</sup> which is consistent with previous studies on the tumor-promoting function of MLACs.<sup>[8]</sup> Our RNA-seq analysis also indicated that there were increased expression levels of other cytokines and chemokines previously detected in MLACs. These include *CCL17*, which can directly stimulate cancer cell proliferation,<sup>[8,27]</sup> and *CCL22*, a cytokine that attracts regulatory T cells.<sup>[28]</sup> These may be auxiliary drivers of tumor growth and immunosuppression. These results further highlight the ability of MLACs to employ different mechanisms to promote tumor development and progression.

Proteomic analysis showed that CD11c expression levels were 34.2-fold higher in MLACs than in MDSCs, but transcriptomic analysis showed a less than two-fold difference (Table S4, Supporting Information), suggesting that CD11c may be regulated primarily at the protein level. CD11c protein levels are known to be correlated with pro-inflammatory cytokines such as IL-12<sup>[29]</sup> and TNF- $\alpha$ <sup>[29,30]</sup> and the presence of damage-associated molecular patterns.<sup>[31]</sup> Because the TME is associated with a chronic inflammatory state, the secretion of many inflammatory cytokines is controlled in a context-dependent manner. This potentially explains why not all MLACs are CD11c-positive and the proportion of CD11c-positive MLACs is not constant. MLACs seem to overlap with conventional dendritic cells with respect to expression of MHCII and CD11c. Although the majority of conventional dendritic cells are F4/80<sup>+</sup>, F4/80<sup>-</sup> subsets of dendritic cells have also been reported.<sup>[32–34]</sup> In line with our scRNA-seq analysis results indicating an association of MLACs with monocyte cell populations, previous studies have also shown that monocytes can upregulate CD11c expression in response to inflammatory stimuli, but did not differentiate nor obtain the antigen presentation activity of dendritic cells.<sup>[35]</sup> This previous work suggests that the observed cells might be MLACs. Furthermore, membrane proteome analysis showed that MLACs have high expression levels of several MHCII subunits, such as H2-Ab1, H2-Eb1, H2-

Aa, and H2-Dma. The H2-Ab1 antibody clone used in this study could detect multiple MHC Class II I-Ab alloantigens. However, this antibody did not detect MDSCs. It is possible that the previously reported CD11b<sup>+</sup>F4/80<sup>-</sup> tumor-infiltrating cell population that highly expressed MHCII<sup>[36]</sup> may have been MLACs. Hence, MLACs may already be recognized as a poorly characterized subset of tumor-infiltrating myeloid cells. Further studies are required to determine the relationship between MLACs and dendritic cells, as well as to investigate if MLACs possess antigen-presenting capabilities. This study will contribute to a better understanding of the complexity of tumor-infiltrating cell populations.

The scRNA-seq analysis and validation of surface markers have highlighted the heterogeneity within MLACs. Thus, we were unable to identify marker proteins that specifically label the entire MLAC population, with uncharacterized subsets remaining among Adh-MLACs. Only 13% to 16% of Adh-MLACs co-expressed both H2-Ab1 and CD11c, with some populations of Adh-MLACs expressing only one marker. Therefore, when we sorted using only one marker, H2-Ab1<sup>-</sup> and CD11c<sup>-</sup> cells could have been mixed with a considerable number of MLACs. Nevertheless, H2-Ab1<sup>-</sup> and CD11c<sup>-</sup> cells did not show clear MLAC properties, except that they had slightly higher growth-promoting activity than MDSCs (Figure 4C). The “residual” MLAC population is potentially very minute among the CD11b<sup>+</sup>F4/80<sup>-</sup> population, as they were hardly detected by qRT-PCR analysis (Figure 4B). Because the use of either marker would be sufficient to isolate and label cells with MLAC characteristics, utilizing H2-Ab1<sup>+</sup> and CD11c<sup>+</sup> subsets sorted directly from tumor-extracted cells will facilitate further investigation of MLACs. Additional studies are needed to more deeply explore the other CD11b<sup>+</sup>F4/80<sup>-</sup> Adh-MLAC subpopulations and determine the relationship and potential differences between H2-Ab1<sup>+</sup> and CD11c<sup>+</sup> MLAC subsets.

Although this study focused on membrane proteins, cytosolic and nuclear proteins may be excellent markers for isolating specific cell populations. Investigating these proteins in future studies may identify marker proteins that enable the isolation of the entire MLAC population from tumor-extracted cells. Investigating whether MLAC also exists in humans is important in understanding tumor immunity. Humans possess several CD11c and MHCII-expressing cell subpopulations.<sup>[37]</sup> Human orthologs for all the MLAC markers such as HLA-DQB2 for H2-Ab1<sup>[38]</sup> exist and can be used as a framework to determine the MLAC counterpart in humans. In the meantime, studies using the H2-Ab1<sup>+</sup> and CD11c<sup>+</sup> subsets are expected to provide sufficient information to advance our understanding of MLACs, leading to the development of therapeutic strategies to inhibit or delay the formation of an immunosuppressive TME. Further in vivo analysis is required to investigate the universality of MLAC markers and the MLAC gene signature across different tumor models and tissues, such as spleen, blood, and bone marrow. The dynamics and pattern of MLAC accumulation in early tumors could also be determined using a mouse model with fluorescent reporters, such as Kikume Green-Red, which changes color from green to red upon violet light irradiation.<sup>[39]</sup> The spleen or bone marrow may be irradiated following tumor formation, and the presence of MLACs within the photoconverted cells can be detected to determine the origin, tissues of accumulation, and fate of MLACs.

## 4. Experimental Section

**Cell Culture:** A C57BL mouse-derived LLC cell line was obtained from the American Type Culture Collection (ATCC; Manassas, VA, USA). Firefly luciferase-expressing LLC cell line (LLC/Fluc) which was established in a previous study<sup>[8]</sup> were grown in Dulbecco's Modified Eagle's Medium (DMEM; Gibco Thermo Fisher Scientific, Waltham, MA, USA) supplemented with 5% fetal bovine serum (FBS; Gibco), 100 units mL<sup>-1</sup> penicillin, and 100 units mL<sup>-1</sup> streptomycin (Nacalai Tesque, Kyoto, Japan) in a 5% CO<sub>2</sub> incubator at 37 °C. The cells were regularly checked for mycoplasma contamination using a mycoplasma detection kit (Takara Bio, Shiga, Japan).

**Mice:** Male B6(Cg)-Tyr<sup>c-2l</sup>/J (B6 albino) mice were obtained from Charles River Laboratories, Japan (Yokohama, Japan). All mice were housed in specific pathogen-free conditions in the animal facilities at the Tokyo Institute of Technology. Animal experiments were performed with the approval of the Animal Experiment Committees of the Tokyo Institute of Technology (no. D2020008) and in accordance with the Ethical Guidelines for Animal Experimentation of the Tokyo Institute of Technology.

**Subcutaneous Tumor Model:** LLC cells (1 × 10<sup>6</sup> cells 20 μL<sup>-1</sup>) were mixed with an equal volume of Geltrex (Thermo Fisher Scientific) and injected subcutaneously into the ventral part of the hind limb of 6 to 9-week-old B6 albino mice.

**Isolation of MLACs and MDSCs:** Subcutaneous tumors 15–20 mm in diameter (<2000 mm<sup>3</sup> in volume) were resected, minced using a scalpel blade, and digested in RPMI (Gibco) supplemented with 2.6 U Liberase DH (Roche Applied Science, Indianapolis, IN, USA) containing 2% FBS at 37 °C. Digested tumor fragments were filtered through a 40 μm pore size cell strainer (Greiner Bio-One, Kremsmünster, Austria) to obtain single-cell suspensions, then treated with Pharm Lyse solution (BD Biosciences, Franklin Lakes, NJ, USA) for 10 min at room temperature to lyse red blood cells. Adherent and non-adherent cells were obtained by adhesion-based separation following methods described previously.<sup>[8]</sup> Briefly, obtained cell suspensions (1 × 10<sup>7</sup> cells/100 mm dish) were cultured in 2% FBS-RPMI for 25 min, and adherent cells were prepared after washing three times with phosphate-buffered saline (PBS) containing 0.68 mM ethylenediaminetetraacetic acid (EDTA) and collected with a cell scraper in PBS containing 2.5 mM EDTA. Non-adherent cells were prepared from the supernatant fraction after two 25 min incubations in plastic dishes. Cell suspensions in fluorescence-activated cell sorting (FACS) buffer (PBS containing 1.2 mM EDTA and 5% FBS) were sorted for MLACs, MDSCs, and TAMs using FACSaria (BD Biosciences) or MoFloXDP (Beckman Coulter, Brea, CA, USA) as previously described.<sup>[8]</sup>

**Flow Cytometry Analysis:** Cells were blocked with anti-FcγRII/III (BioLegend, San Jose, CA, USA, 93, 1:200) for 25 min at 4 °C and stained with fluorescent-conjugated antibodies for 30 min at 4 °C. Cells were washed with FACS buffer and analyzed using the iCyt EC800 (Sony Biotechnology, Tokyo, Japan). Flow cytometry results were analyzed and mean MFI values were measured using FlowJo (TreeStar, Ashland, OR, USA). The monoclonal antibodies used for flow cytometry analysis were as follows: CD11b (M1/70, 1:200), Ly6G (1A8, 1:100), Ly6C (HK1.4, 1:100), CD11c (N418, 1:100), H2-Ab1 (AF6-120.1, 1:50), Mgl2 (URA-1, 1:100), CD209a (MMD3, 1:50), Klr1d1 (18D3, 1:100) CD8 m (53.6-7, 1:100) (all from BioLegend), F4/80 (Bio-Rad, Hercules, CA, USA, C1:A3-1, 1:50), and Gr-1 (RB6-8C5, 1:100) and Chicken Anti-rat (polyclonal, 1:250) (both from eBioscience, San Diego, CA, USA).

**qRT-PCR:** Total RNA was extracted from FACS-sorted cells using the RNeasy Mini Kit (Qiagen, Hilden, Germany). RNA concentration was determined using a Nanodrop instrument (Thermo Fisher Scientific), and then samples were reverse transcribed into cDNA using ReverTra Ace (Toyobo, Osaka, Japan) with Oligo(dt)<sub>20</sub> primers (Toyobo). Next, qRT-PCR amplification was performed with the Thunderbird SYBR qPCR mix (Toyobo) using the TP800 Thermal Cycler Dice Real Time System (Takara Bio). The relevant qRT-PCR primer sequences were as follows: Actin-F: 5'-GGCTACAGCTTACCACCAC-3', Actin-R: 5'-TACTCCTGCTTGCTGATCCAC-3', Mgl2-F: 5'-ACTTCCAGAACTTGGAGCGG-3', Mgl2-R: 5'-CTGGGAAGGAAGTGTAGAGCA-3', CD209a-F: 5'-TTCACCTCTGACTCTCAGTTTCAT-3', CD209a-R: 5'-

GGTGTCAATCCAGCCGTCAT-3', CD74-F: 5'-CCGAAATCTGCCAAA-CCTGTG-3', CD74-R: 5'-CAGGCCCAAGGAGCATGTTA-3', Klr1d1-F: 5'-CAGGAAGTTTCTGAATGCTGTGT-3', Klr1d1-R: 5'-TGGATTGGGGCTGAAGAAGG-3'. The expression levels of genes of interest were normalized to actin gene expression.

**RNA-Seq Analysis:** RNA samples were pooled from 10 tumor-bearing mice. The RNA integrity number was assessed using capillary gel electrophoresis with an Agilent 2100 Bioanalyzer instrument (Agilent Technologies, Santa Clara, CA, USA) by Hokkaido System Science (Sapporo, Japan). Total RNA was treated with DNase (Qiagen), then library preparation was performed using the TruSeq mRNA Stranded Library Preparation Kit (Illumina, San Diego, CA, USA) and samples were sequenced using Illumina HiSeq at a depth of at least 20 million reads per sample.

Reads were aligned to the UCSC mm10 Mus Musculus reference genome through HISAT2.<sup>[40]</sup> Raw transcript count was obtained using Subread (FeatureCount).<sup>[41]</sup> Normalization of counts and determination of differentially expressed genes were performed through the R Noiseq package.<sup>[42]</sup> GSEA was performed by referencing the Molecular Signatures Database.<sup>[43]</sup> Plasma membrane encoding genes were determined through GO analysis from the University of California Santa Cruz Genome Browser database.<sup>[44]</sup>

**scRNA-Seq Dataset Processing:** The dataset (Accession number: GSE121861 and GSE121478) was downloaded from Gene Expression Omnibus.<sup>[15]</sup> The raw counts were loaded in a Rstudio project session and analyzed by Seurat Ver 3.0.<sup>[45]</sup> Ptpcr (CD45)-expressing cells were selected for further analysis. Raw counts were normalized, and Uniform Manifold Approximation and Projection (UMAP) clustering analysis was performed to identify major cell clusters. For cell subset analyses, clusters with high Itgam (CD11b) and low Adgre1 (F4/80) expression levels were grouped together and reanalyzed using UMAP. Specific markers for each cluster were identified using the "FindAllMarkers" function. MLAC and MDSC cluster identities were determined using known marker expression. Heatmaps and violin plots were generated using built-in Seurat commands.<sup>[46]</sup>

**Peptide Preparation and Proteomic Analysis:** Membrane proteins were isolated from sorted MDSCs and MLACs using the Mem-Per Plus membrane protein extraction kit (Thermo Fisher Scientific) according to the manufacturer's instructions. Membrane proteins were dissolved in a solubilization buffer and stored at -80 °C. Proteins were reduced with 1 M dithiothreitol (DTT) and alkylated using 1 M iodoacetamide (Fujifilm Wako Pure Chemical, Osaka, Japan). Samples were then diluted fivefold with 50 mM ammonium bicarbonate buffer and digested as previously described.<sup>[47]</sup> Briefly, proteins were digested with Trypsin/Lysyl endopeptidase mix (Trypsin/Lys-C, Mass Spectrometry grade, Promega, Madison, WI, USA) (0.5 μg/50 μg protein) for 3 h at 25 °C. Finally, additional Trypsin/Lysyl endopeptidase mix (1 μg/50 μg protein) was added, and samples were digested overnight at 37 °C. Detergents were removed through precipitation with ethyl acetate and 0.5% trifluoroacetic acid.

Desalting of peptides was performed through StageTip (GL Sciences, Tokyo, Japan) and was analyzed using a nanoLC-mass spectrometer (Quadrupole-Orbitrap, Thermo Fisher Scientific). MS data were processed using Proteome Discoverer 3.0 (Thermo Fisher Scientific) and protein IDs were identified through the murine Uniprot protein database.<sup>[48]</sup> Differentially expressed proteins were identified through calculation of fold-change and *p*-values less than 0.05 were considered significant.

**RRHO Analysis:** Gene expression counts from RNA-seq data were tabulated with peptide counts from LC-MS/MS by matching the corresponding gene IDs with protein IDs. The input score was calculated using the fold-change and *p*-value of expression from the RNA-seq and proteomics analyses by calculating Cohen's D.<sup>[24]</sup> Detection and ranking of top correlated candidates were performed through RRHO analysis. The segmented heatmap was generated through the RRHO2 R package.<sup>[49]</sup>

**Co Culture Assay:** LLC/Fluc cells (2.4 × 10<sup>4</sup>/1.44 mL medium) were seeded into 24-well culture plates (Greiner Bio-One) and cocultured with 3.6 × 10<sup>4</sup> myeloid cells sorted from tumors. After culturing for 48 h at 37 °C, LLC/Fluc cells were lysed with Passive Lysis Buffer (Promega), and then luciferase activity was measured using a Luciferase Assay Kit (Promega) and luminometer (GL-210A, Microtec, Chiba, Japan).

**T Cell Inhibition Assay:** CD8<sup>+</sup> T cells were sorted from splenocytes of healthy C57BL/6 mice and labeled with 2.5 μM CFSE (Thermo Fisher Scientific) for 10 min. The cells were then washed and resuspended in RPMI supplemented with 10% FBS and 50 μM β-mercaptoethanol. T cells (5 × 10<sup>4</sup>) were seeded into each well of a 96-well U-bottom plate (Corning, Corning, NY, USA) that was pre-coated with anti-CD3ε (0.75 μg mL<sup>-1</sup>; BioLegend, 145-2C11) and anti-CD28 (2 μg mL<sup>-1</sup>; BioLegend, 37.51) for stimulated set-ups. T cells were then cocultured with sorted MLACs or MDSCs and incubated for 3 days. Cells were then collected, blocked with anti-mouse CD16/32 (BioLegend, 93, 1:200), and stained with anti-CD8 (BioLegend, 53-6.7, 1:100). T cell proliferation was assessed by flow cytometry (iCyt EC800) and division indices were calculated using FlowJo.

**Statistical Analysis:** For differential expression analysis, R Noiseq assumes a multinomial distribution of gene expression to simulate technical replicates and to calculate *p*-values. Differentially expressed genes from Noiseq analysis were determined with the threshold: *q* = 0.8. Continuous variables are presented as mean ± standard deviation (SD). For proteome analysis, *p*-values less than 0.05 were considered statistically significant. For qRT-PCR, expression levels of target genes were normalized to actin, and fold-change expression was compared. For coculture assay, the relative growth of setups was compared. For T cell inhibition assay, the division indices of cells of interest were compared.

The statistical significance between the two groups was determined by unpaired Student's *t*-test. *p*-values < 0.05 were considered statistically significant. The sample size was indicated for each experiment in the figure legend. Bar graphs were generated and statistical analysis was carried out using GraphPad Prism software (v.9.5, GraphPad Software, La Jolla, CA, USA).

## Supporting Information

Supporting Information is available from the Wiley Online Library or from the author.

## Acknowledgements

The authors are thankful for the technical assistance of the FACS Core Laboratory, Institute of Medical Science, Tokyo University and the Joint Research Laboratory, Faculty of Medicine, Keio University for cell sorting. The authors would also like to acknowledge the Open Research Facilities for Life Science and Technology. This study was supported by the Princess Takamatsu Cancer Research Fund (SKK), the Naito Foundation (SKK), the NOVARTIS Foundation of Japan (SKK), and MEXT Quantum Leap Flagship Program (MEXT QLEAP) Grant Number JPMXS0120330644. We thank J. Iacona, Ph.D., from Edanz for editing a draft of this manuscript.

## Conflict of Interest

The authors declare no conflicts of interest.

## Author Contributions

J.C.C.S., T.S., T.K., and S.K.K. contributed to experimental design and data interpretation. J.C.C.S. and S.T. maintained and isolated samples from the mouse tumor model. JCCS performed the experiments. J.C.C.S., D.O., K.H., and GK performed the transcriptome analysis. J.C.C.S., T.N., and H.T. performed the proteome analysis. J.C.C.S., T.K., and S.K.K. wrote the manuscript.

## Data Availability Statement

The data that support the findings of this study are openly available in DNA Data Bank of Japan (DDBJ) at <https://www.ddbj.nig.ac.jp/index-e.html>, reference number (DRA015617).

## Keywords

cancer microenvironment, cell surface markers, myeloid cells, tumor immunology

Received: April 26, 2023

Revised: October 11, 2023

Published online: November 20, 2023

- [1] D. I. Gabrilovich, *Cancer Immunol. Res.* **2017**, *5*, 3.
- [2] X. Chen, M. Song, B. Zhang, Y. Zhang, *Oxid Med Cell Longev* **2016**, *2016*, 1580967.
- [3] J.-I. Youn, S. Nagaraj, M. Collazo, D. I. Gabrilovich, *J. Immunol.* **2008**, *181*, 5791.
- [4] V. Bronte, S. Brandau, S.-H. Chen, M. P. Colombo, A. B. Frey, T. F. Greten, S. Mandruzzato, P. J. Murray, A. Ochoa, S. Ostrand-Rosenberg, P. C. Rodriguez, A. Sica, V. Umansky, R. H. Vonderheide, D. I. Gabrilovich, *Nat. Commun.* **2016**, *7*, 12150.
- [5] C. A. Corzo, T. Condamine, L. Lu, M. J. Cotter, J.-I. Youn, P. Cheng, H.-I. Cho, E. Celis, D. G. Quiceno, T. Padhya, T. V. Mccaffrey, J. C. Mccaffrey, D. I. Gabrilovich, *J. Exp. Med.* **2010**, *207*, 2439.
- [6] K. Movahedi, D. Laoui, C. Gysemans, M. Baeten, G. Stangé, J. van den Bossche, M. Mack, D. Pipeleers, P. In't Veld, P. De Baetselier, *Cancer Res.* **2010**, *70*, 5728.
- [7] S. Qiu, L. Deng, X. Liao, L. Nie, F. Qi, K. Jin, X. Tu, X. Zheng, J. Li, L. Liu, Z. Liu, Y. Bao, J. Ai, T. Lin, L. Yang, Q. Wei, *Cancer Sci.* **2019**, *110*, 2110.
- [8] T. Tsubaki, T. Kadonosono, S. Sakurai, T. Shiozawa, T. Goto, S. Sakai, T. Kuchimaru, T. Sakamoto, H. Watanabe, G. Kondoh, S. Kizaka-Kondoh, *Oncotargets Ther.* **2018**, *9*, 11209.
- [9] H. Alshetaiwi, N. Pervolarakis, L. L. McIntyre, D. Ma, Q. Nguyen, J. A. Rath, K. Nee, G. Hernandez, K. Evans, L. Torosian, A. Silva, C. Walsh, K. Kessenbrock, *Sci Immunol* **2020**, *5*, eaay6017.
- [10] V. Kumar, S. Patel, E. Tcyganov, D. I. Gabrilovich, *Trends Immunol.* **2016**, *37*, 208.
- [11] R. Zilionis, C. Engblom, C. Pfirschke, V. Savova, D. Zemmour, H. D. Saaticioglu, I. Krishnan, G. Maroni, C. V. Meyerovitz, C. M. Kerwin, S. Choi, W. G. Richards, A. De Rienzo, D. G. Tenen, R. Bueno, E. Levantini, M. J. Pittet, A. M. Klein, *Immunity* **2019**, *50*, 1317.
- [12] R. Bucala, I. Shachar, *Mini Rev Med Chem* **2014**, *14*, 1132.
- [13] L. Heger, T. P. Hofer, V. Bigley, I. J. M. de Vries, M. Dalod, D. Dudziak, L. Ziegler-Heitbrock, *Front Immunol* **2020**, *11*, 559166.
- [14] D. Binns, E. Dimmer, R. Huntley, D. Barrell, C. O'donovan, R. Apweiler, *Bioinformatics* **2009**, *25*, 3045.
- [15] M. P. Kumar, J. Du, G. Lagoudas, Y. Jiao, A. Sawyer, D. C. Drummond, D. A. Lauffenburger, A. Raue, *Cell Rep.* **2018**, *25*, 1458.
- [16] T. Moriguchi, M. Hamada, N. Morito, T. Terunuma, K. Hasegawa, C. Zhang, T. Yokomizo, R. Esaki, E. Kuroda, K. Yoh, T. Kudo, M. Nagata, D. R. Greaves, J. D. Engel, M. Yamamoto, S. Takahashi, *Mol. Cell. Biol.* **2006**, *26*, 5715.
- [17] V. Kumar, L. Donthireddy, D. Marvel, T. Condamine, F. Wang, S. Lavilla-Alonso, A. Hashimoto, P. Vonteddu, R. Behera, M. A. Goins, C. Mulligan, B. Nam, N. Hockstein, F. Denstman, S. Shakamuri, D. W. Speicher, A. T. Weeraratna, T. Chao, R. H. Vonderheide, L. R. Languino, P. Ordentlich, Q. Liu, X. Xu, A. Lo, E. Puré, C. Zhang, A. Loboda, M. A. Sepulveda, L. A. Snyder, D. I. Gabrilovich, *Cancer Cell* **2017**, *32*, 654.
- [18] P. R. Gielen, B. M. Schulte, E. D. Kers-Rebel, K. Verrijp, S. A. J. F. H. Bossman, M. Ter Laan, P. Wesseling, G. J. Adema, *Neuro Oncol* **2016**, *18*, 1253.
- [19] F. Veglia, M. Perego, D. Gabrilovich, *Nat. Immunol.* **2018**, *19*, 108.

- [20] M. Sade-Feldman, J. Kanterman, E. Ish-Shalom, M. Elnekave, E. Horwitz, M. Baniyash, *Immunity* **2013**, *38*, 541.
- [21] D. Brusa, M. Simone, P. Gontero, R. Spadi, P. Racca, J. Micari, M. Degiuli, S. Carletto, A. Tizzani, L. Matera, *Int. J. Urol. Off. J. Japanese Urol. Assoc.* **2013**, *20*, 971.
- [22] H. A. Ekiz, T. B. Huffaker, A. H. Grossmann, W. Z. Stephens, M. A. Williams, J. L. Round, R. M. O'connell, *JCI Insight* **2019**, *4*, e126543.
- [23] A. J. Hoogendijk, F. Pourfarzad, C. E. M. Aarts, A. T. J. Tool, I. H. Hiemstra, L. Grassi, M. Frontini, A. B. Meijer, M. Van Den Biggelaar, T. W. Kuijpers, *Cell Rep.* **2019**, *29*, 2505 .
- [24] S. B. Plaisier, R. Taschereau, J. A. Wong, T. G. Graeber, *Nucleic Acids Res.* **2010**, *38*, e169 .
- [25] S. H. Ryu, H. S. Shin, H. H. Eum, J. S. Park, W. Choi, H. Y. Na, H. In, T.-G. Kim, S. Park, S. Hwang, M. Sohn, E.-D. Kim, K. Y. Seo, H.-O. Lee, M.-G. Lee, M. K. Chu, C. G. Park, *Front Immunol* **2022**, *12*, 767037.
- [26] M. L. Varney, S. Singh, A. Li, R. Mayer-Ezell, R. Bond, R. K. Singh, *Cancer Lett* **2011**, *300*, 180.
- [27] F. Zhu, X. Li, S. Chen, Q. Zeng, Y. Zhao, F. Luo, *Med Oncol* **2016**, *33*, 17.
- [28] M. Gobert, I. Treilleux, N. Bendriss-Vermare, T. Bachelot, S. Goddard-Leon, V. Arfi, C. Biota, A. C. Doffin, I. Durand, D. Olive, S. Perez, N. Pasqual, C. Faure, I. Ray-Coquard, A. Puisieux, C. Caux, J.-Y. Blay, C. Ménétrier-Caux, *Cancer Res.* **2009**, *69*, 2000.
- [29] K. Poropatich, D. Dominguez, W.-C. Chan, J. Andrade, Y. Zha, B. Wray, J. Miska, L. Qin, L. Cole, S. Coates, U. Patel, S. Samant, B. Zhang, *J. Clin. Invest.* **2020**, *130*, 3528.
- [30] A. Gutiérrez-Seijo, E. García-Martínez, C. Barrio-Alonso, M. Pareja-Malagón, A. Acosta-Ocampo, M. E. Fernández-Santos, A. Puig-Kröger, V. Parra-Blanco, E. Mercader, I. Márquez-Rodas, J. A. Avilés-Izquierdo, R. Samaniego, *Cancers (Basel)* **2021**, *13*, 3943.
- [31] H. Lee, H. J. Lee, I. H. Song, W. S. Bang, S.-H. Heo, G. Gong, I. A. Park, *In Vivo (Brooklyn)* **2018**, *32*, 1561.
- [32] J. Sheng, Q. Chen, I. Soncin, S. L. Ng, K. Karjalainen, C. Ruedl, *Cell Rep.* **2017**, *21*, 1203.
- [33] A. Hotblack, A. Holler, A. Piapi, S. Ward, H. J. Stauss, C. L. Bennett, *Mol. Ther.* **2018**, *26*, 1471.
- [34] I. Soncin, J. Sheng, Q. Chen, S. Foo, K. Duan, J. Lum, M. Poidinger, F. Zolezzi, K. Karjalainen, C. Ruedl, *Nat. Commun.* **2018**, *9*, 582.
- [35] S. B. Drutman, J. C. Kendall, E. S. Trombetta, *J. Immunol.* **2012**, *188*, 3603.
- [36] W. Huang, Y. Liu, A. Luz, M. Berrong, J. N. Meyer, Y. Zou, E. Swann, P. Sundaramoorthy, Y. Kang, S. Jauhari, W. Lento, N. Chao, L. Racioppi, *Front Immunol* **2021**, *12*, 754083.
- [37] S. K. Wculek, F. J. Cueto, A. M. Mujal, I. Melero, M. F. Krummel, D. Sancho, *Nat. Rev. Immunol.* **2020**, *20*, 7.
- [38] J. A. Blake, J. T. Eppig, J. A. Kadin, J. E. Richardson, C. L. Smith, C. J. Bult, *Nucleic Acids Res.* **2017**, *45*, D723.
- [39] H. Tsutsui, S. Karasawa, H. Shimizu, N. Nukina, A. Miyawaki, *EMBO Rep.* **2005**, *6*, 233.
- [40] J. Siren, N. Valimaki, V. Mäkinen, *IEEE/ACM Trans. Comput. Biol. Bioinforma.* **2014**, *11*, 375.
- [41] Y. Liao, G. K. Smyth, W. Shi, *Nucleic Acids Res.* **2019**, *47*, e47.
- [42] S. Tarazona, P. Furió-Tarí, D. Turrà, A. Di Pietro, M. J. Nueda, A. Ferrer, A. Conesa, *Nucleic Acids Res.* **2015**, *43*, e140.
- [43] A. Liberzon, A. Subramanian, R. Pinchback, H. Thorvaldsdóttir, P. Tamayo, J. P. Mesirov, *Bioinformatics* **2011**, *27*, 1739.
- [44] W. J. Kent, C. W. Sugnet, T. S. Furey, K. M. Roskin, T. H. Pringle, A. M. Zahler, *Genome Res.* **2002**, *12*, 996.
- [45] T. Stuart, A. Butler, P. Hoffman, C. Hafemeister, E. Papalexi, W. M. Mauck, Y. Hao, M. Stoeckius, P. Smibert, R. Satija, *Cell* **2019**, *177*, 1888 .
- [46] A. Butler, P. Hoffman, P. Smibert, E. Papalexi, R. Satija, *Nat. Biotechnol.* **2018**, *36*, 411.
- [47] F. Deschoenmaeker, S. Mihara, T. Niwa, H. Taguchi, K.-I. Wakabayashi, T. Hisabori, *Plant Cell Physiol.* **2018**, *59*, 2432.
- [48] Y. Wang, Q. Liu, Y. Liu, G. Li, G. Xia, M. Wang, *PLoS Biol.* **2021**, *65*, 19.
- [49] K. M. Cahill, Z. Huo, G. C. Tseng, R. W. Logan, M. L. Seney, *Sci. Rep.* **2018**, *8*, 9588.